Momentum Distribution and Renormalization Factor in Sodium and the Electron Gas

Simo Huotari,[1,2] J. Aleksi Soininen,[2] Tuomas Pylkkänen,[1,2] Keijo Hämäläinen,[2] Arezki Issolah,[3] Andrey Titov,[4] Jeremy McMinis,[5] Jeongnim Kim,[5] Ken Esler,[5] David M. Ceperley,[5] Markus Holzmann,[6] and Valerio Olevano[4]

[1]*European Synchrotron Radiation Facility, B.P. 220, F-38043 Grenoble, France*
[2]*Department of Physics, P.O. Box 64, FI-00014, University of Helsinki, Finland*
[3]*Université de Tizi-Ouzou, Campus de Hasnaoua, 15000 Tizi-Ouzou, Algeria*
[4]*Institut Néel, CNRS and UJF, F-38042 Grenoble, France*
[5]*Department of Physics and NCSA, University of Illinois at Urbana-Champaign, Urbana, Illinois 61801, USA*
[6]*LPTMC, UPMC-CNRS, Paris, France, and LPMMC, UJF-CNRS, F-38042 Grenoble, France*

(Received 23 June 2010; published 19 August 2010)

We present experimental and theoretical results on the momentum distribution and the quasiparticle renormalization factor in sodium. From an x-ray Compton-profile measurement of the valence-electron-momentum density, we derive its discontinuity at the Fermi wave vector. This yields an accurate measure of the renormalization factor that we compare with quantum Monte Carlo and G_0W_0 calculations performed both on crystalline sodium and on the homogeneous electron gas.

DOI: 10.1103/PhysRevLett.105.086403 PACS numbers: 71.10.−w, 02.70.Ss, 71.20.Dg, 78.70.Ck

Introduction.—The homogeneous electron gas (HEG), also known as jellium, is one of the most fundamental models in condensed matter physics [1]. It is one of the simplest many-body systems that can describe several properties of real solids, especially the alkali metals. For almost half a century, the accurate description of many-body correlation effects has challenged quantum many-body theory, and HEG is the canonical workbench to test different theoretical methods [2–8]. Although the analytic solution of the many-body problem in HEG is still unknown, today quantum Monte Carlo (QMC) calculations provide the most reliable results on, e.g., the correlation energy. The situation is less clear concerning spectroscopic quantities such as the momentum distribution $n(p)$. The accuracy of the theoretical methods in this respect is not well understood, with different approaches yielding a wide range of results. This fundamental issue remains unresolved, mainly due to a lack of accurate and bulk-sensitive experimental probes for comparison with theory.

Experimentally, one of nature's closest realizations of HEG is formed by the valence electrons in alkali metals, especially Na. Here, we present very accurate experimental and theoretical results on the electron-momentum distribution of Na. The single occupied valence band of Na has an almost spherical Fermi surface (FS), and its properties in ambient conditions with a density parameter $r_s = 3.99$ can be directly compared with theoretical results on HEG. In particular, we obtain a precise experimental reference value for the quasiparticle renormalization factor Z_{k_F}, which characterizes the discontinuity of the momentum distribution at the FS [1]. From the Compton profile (CP) measured by inelastic x-ray scattering experiments on bulk sodium, we derive $n(p)$ and obtain $Z_{k_F}^{\mathrm{Na}} = 0.58(7)$. Our experiment provides a clear and direct observation of the discontinuity at the FS.

We compare our experimental results to theoretical calculations using QMC and G_0W_0 methods, for both HEG and Na, including the electron-electron interaction and band-structure effects. Our calculations confirm the jellium-like behavior of Na and allow us to quantify the small deviations from HEG. Finally, we compare the results with other many-body approximations applied to HEG in literature [2–8]. Unless explicitly specified, we use atomic units (a.u.).

Theory.—The momentum distribution per spin state $n(p)$ (see Fig. 1) is one of the basic many-body observables where the Pauli principle for fermions is directly visible. It is the probability to observe an electron with momentum p. For a noninteracting Fermi gas at zero temperature, $n(p)$ is 1 for p below the Fermi momentum p_F and 0 above, i.e., $n(p) = \theta(p_F - p)$ with a discontinuity $\zeta = n(p_F^-) - n(p_F^+) = 1$ occurring at the FS. For a noninteracting crystalline system, the electrons occupy Bloch wave functions,

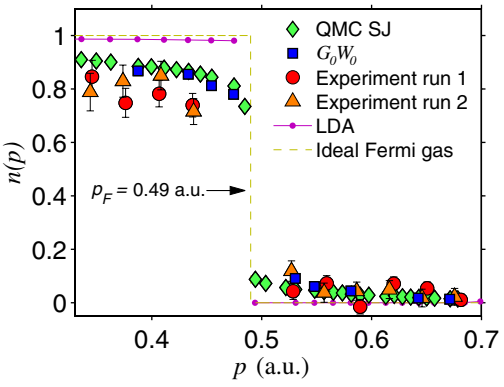

FIG. 1 (color online). The momentum distribution of Na determined by experiment, QMC SJ, G_0W_0, and LDA calculations. The ideal-Fermi gas step function is also shown.

$\phi_{\nu\mathbf{k}}(\mathbf{r}) = \sum_{\mathbf{G}} \tilde{\phi}^{\mathbf{G}}_{\nu\mathbf{k}} e^{i(\mathbf{k}+\mathbf{G})\mathbf{r}}$, where $\mathbf{k}$ is the crystal momentum, ν is the band index, and $\mathbf{G}$ are reciprocal lattice vectors. For systems like Na with one valence band ($\nu = 1$) whose Fermi surface is entirely contained within the first Brillouin zone (1BZ), the band structure reduces the discontinuity of the $n(p)$, $\zeta = |\tilde{\phi}^{\mathbf{G}=0}_{\nu=1,\mathbf{k}_F}|^2 < 1$. From a density-functional theory calculation within the local-density approximation (LDA) for Na, we obtain $\zeta^{\mathrm{Na}}_{\mathrm{LDA}} = 0.98(1)$. The calculated valence band is an almost perfect parabola, its wave function is nearly isotropic, and its FS deviates from a perfect sphere by only 0.2%, leading to a further, albeit small, reduction of the discontinuity when $n(p)$ is orientationally averaged.

Many-body effects introduce a much larger reduction of the discontinuity at the FS, known as the quasiparticle renormalization factor $Z_{\mathbf{k}_F}$. Theoretical predictions for $Z_{\mathbf{k}_F}$ using different approximations range from 0.45 to 0.79 for the density considered (see Table I). In general, $Z_{\mathbf{k}_F}$ is related to the self-energy $\Sigma_{\nu,\nu}(k,\omega)$ via $Z_{\mathbf{k}_F} = [1 - \partial\Sigma_{1,1}(\mathbf{k}_F,\omega)/\partial\omega|_{\omega=\epsilon_F}]^{-1}$, $\Sigma = \Sigma^{e\text{-}e} + \Sigma^{e\text{-ph}}$ containing the electron-electron interactions $\Sigma^{e\text{-}e}$ and the electron-phonon effects $\Sigma^{e\text{-ph}}$. For HEG the discontinuity in $n(p)$ is $\zeta_{\mathrm{HEG}} = Z_{k_F}$. In a jelliumlike system such as Na, band-structure effects and many-body correlations can be factorized so that $\zeta_{\mathrm{Na}} = |\tilde{\phi}^{\mathbf{G}=0}_{\nu=1,\mathbf{k}_F}|^2 Z_{\mathbf{k}_F}$ with $Z_{\mathbf{k}_F}$ very close to the value for HEG at the same density, if phonon effects can be neglected.

To determine $Z_{\mathbf{k}_F}$ theoretically, we performed pseudopotential diffusion QMC [9,10] calculations of bulk sodium based on a Slater-Jastrow (SJ) wave function using the QMCPACK code, and more precise calculations using backflow (BF) for HEG. In addition, we have done a non-self-consistent (one-shot) G_0W_0 calculation [2] starting from LDA using the ABINIT code. Within both QMC and G_0W_0 methods, pseudopotentials are used to describe the core electrons, based on a regular static lattice for the ions, neglecting effects due to electron-phonon coupling.

TABLE I. Our results for ζ and Z_{k_F} of Na and HEG at $r_s = 4.0$: experimental value compared to G_0W_0, QMC SJ and QMC BF. Various theoretical values of HEG from literature are also quoted. [Effective-potential expansion (EPX), Fermi hypernetted chain (FHNC).]

Technique	ζ^{Na}	$Z^{\mathrm{Na}}_{k_F}$	$Z^{\mathrm{HEG}}_{k_F}$
Experiment	0.57(7)	0.58(7)	
QMC SJ	0.68(2)	0.70(2)	0.69(1)
QMC BF			0.66(2)
G_0W_0	0.64(1)	0.65(1)	0.64 [2]
GW [6]			0.793
RPA (on shell) [4,5]			0.45
expS_2 [4]			0.59
EPX [8]			0.61
Lam [5]			0.615
FHNC [7]			0.71

Whereas core correlation effects only give smooth corrections that do not influence the value of the renormalization factor, electron-phonon coupling may lead to a further decrease of $Z_{\mathbf{k}_F}$. However, since the phonon Debye frequency ω_D is small compared to the Fermi energy, the main effects are expected only within a narrow momentum region around p_F, with $\delta p/p_F \lesssim \omega_D/p_F^2 \approx 10^{-2}$, beyond the resolution of the experiment. The static approximation and the use of pseudopotential should thus be sufficient to obtain the value of $Z_{\mathbf{k}_F}$, whereas they may be less accurate to predict the CP itself.

Experiment.—A unique bulk-sensitive probe of the $n(p)$ is offered by Compton scattering of x rays [11]. The experiment measures the spectra of x rays scattered by an electron system. When the energy transferred to the electron is much larger than its binding energy, the so-called impulse approximation is valid and the measured spectrum is related to the CP, which in isotropic average normalized to one electron is

$$J(q) = \frac{3}{8\pi p_F^3} \int_{4\pi} d\Omega \int_{|q|}^{\infty} p n(\mathbf{p}) dp. \tag{1}$$

Here q is the component of the ground-state momentum of the electron projected onto the scattering vector. Assuming an isotropic system, $n(p)$ can thus be extracted by a differentiation of the CP,

$$n(p) = -\frac{2p_F^3}{3p} \frac{dJ(q)}{dq}\bigg|_{q=p}. \tag{2}$$

For the noninteracting HEG the CP is an inverted parabola $J(q) = \frac{3}{4p_F^3}(p_F^2 - q^2)$ for $q < p_F$ and vanishes for $q > p_F$. Many-body effects promote a part of the electrons from below to above p_F. The CP, while being always continuous, will have a discontinuity in the first derivative at p_F. Measuring the CP accurately allows the extraction of $n(p)$ by using Eq. (2). The determination of Z_{k_F} via x-ray Compton scattering has been a long-standing goal of many scientists [11]. The simultaneous requirements of extremely high momentum resolution and statistical accuracy as well as difficulties in separating band-structure and correlation effects have made such attempts difficult, leading to anomalously low values of, e.g., $Z^{\mathrm{Li}}_{k_F} = 0.1(1)$ for Li ($r_s = 3.25$) [12]. Promising results were given for Al ($r_s = 2.07$) [13] by comparisons with an analytical model of $n(p)$ with an adjustable Z_{k_F} [12], giving the best agreement with $Z^{\mathrm{Al}}_{k_F} \approx 0.7$. This determination, however, assumed a specific shape of $n(p)$ and thus was not model independent. Our choice of a HEG-like system of Na combined with ultrahigh resolution measurements allows us to accurately determine the $n(p)$ and $Z^{\mathrm{Na}}_{k_F}$ in a model-independent way.

The experiments were performed at the beam line ID16 [14] of the European Synchrotron Radiation Facility on polycrystalline Na. The spectrometer was based on a Rowland circle with spherically bent analyzer crystals with a Bragg angle of 89°. The measurements were done

by changing the incident-photon energy E_1 and observing the flux of scattered photons into a fixed scattering angle 2θ at a fixed energy E_2. We used two different configurations to verify the result in two independent ways. In the first experiment (run 1), we used a single Si(555) analyzer crystal, $E_2 = 9.9$ keV, $2\theta = 147°$, and $E_1 = 9.9$–11.0 keV. In the second experiment (run 2), two Si(880) analyzers were used, with $E_2 = 12.9$ keV, $2\theta = 149°$, and $E_1 = 12.9$–14.0 keV. The sample was prepared in a glovebox and transported to the beam line within an argon atmosphere and pumped into a vacuum of 10^{-6} mbar. There was no observable degradation of the sample during the experiment. The measured signal was corrected for sample self-absorption as well as changes in the incident-photon flux, and the spectra were measured repeatedly to identify any possible instabilities during the experiment. None were found and the spectra were finally averaged.

The measured spectra as a function of energy transfer are shown in Fig. 2. The Na L edges are seen at 30–60 eV, and K edge at 1.07 keV. Since our interest is in the valence-electron CP, the core contribution has to be subtracted first. Since the impulse approximation is not valid for the core-electron spectra in these experiments, we calculated them with two independent methods: the quasi-self-consistent field (QSCF) approximation [15] and the real-space multiple scattering approach with the FEFFQ code [16,17]. The differences between the results of the two approaches are negligible. The core contribution can then be reliably subtracted from the experimental spectra. The spectra can now be converted into the CP [18]; for each energy transfer we can evaluate the scattering-electron momentum component q, and the measured intensity is related to $J(q)$.

A finite experimental accuracy in the determination of q will introduce a broadening of any sharp features in the experimental data. This uncertainty is caused in the present experiments by the spread of scattering angles of the detected radiation, giving $\Delta q = 0.018$ a.u. (run 1) and $\Delta q = 0.027$ a.u. (run 2) FWHM. Final-state effects [19,20], i.e., the interaction of the scattering electron and the rest of the electron gas, are known to cause further broadening of the measured valence CPs. We calculated the magnitude of this broadening [19], and found it to be effectively an additional Gaussian smoothing of 0.08 a.u. (run 1) and 0.03 a.u. (run 2) (FWHM). This combined with the geometrical resolutions yields effective experimental $\Delta q = 0.08$ a.u. (run 1) and 0.04 a.u. (run 2).

Results and discussion.—The result of the experiment and analysis is the valence CP shown in Fig. 3. For a real metal it generally deviates from the jellium parabola due to two reasons: (i) correlation modifies the $n(p)$ introducing tails for $p > p_F$, and (ii) electron-ion interaction modifies the overall wave function and induces tails for $p > p_F$ due to core orthogonalization and the high-momentum components $\tilde{\phi}^{\mathbf{G}\neq 0}_{\nu\mathbf{k}}$. As discussed above, the valence-electron wave function of Na is fully contained inside 1BZ and is highly free-electron-like, with negligible high-momentum components. The band structure only leads to small ($\lesssim 3\%$) lowering of the momentum distribution for $p < p_F$, as can be seen in the difference between the ideal-Fermi-gas and the LDA results in Fig. 1. Thus we can compare the experimental $n(p)$ to that of HEG after including these corrections.

In Fig. 3, the FS can be directly seen as the discontinuity of the valence CP derivative. From the experimental data we deduce $p_F = 0.49(1)$ a.u. (LDA value 0.481 a.u.). The best determination of ζ is provided by linear fits to the measured points in the immediate vicinity of p_F. An inset to Fig. 3 shows these fits, here for both negative and positive q from run 2. The difference of the slopes for the two sides gives $\zeta^- = 0.59(7)$ and $\zeta^+ = 0.55(7)$, which allows us to quote the average value as $\zeta^{\mathrm{Na}}_{\mathrm{exp}} = 0.57(7)$. The error bar is based on the statistical noise of $J(q)$ and the uncertainty of p_F [cf. Eq. (2)]. Using the pure band-

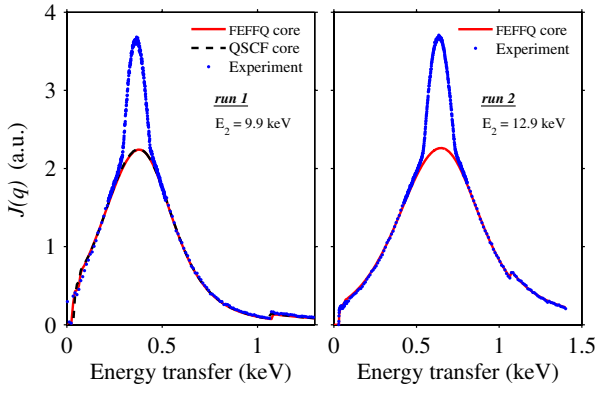

FIG. 2 (color online). The measured x-ray-scattering spectra from Na as a function of energy transfer, for both experimental runs. The experimental spectra consist of overlapping valence and core contributions. Theoretical core contributions are shown for both QSCF and FEFFQ treatments.

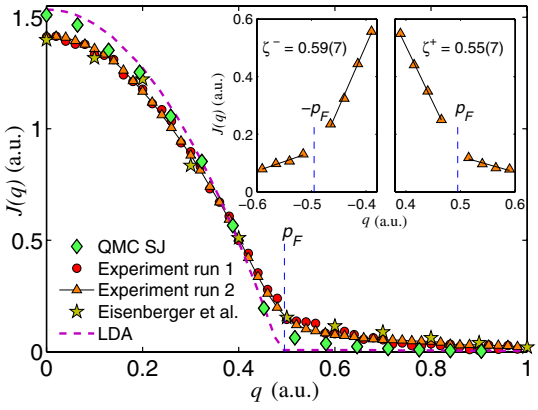

FIG. 3 (color online). The experimental valence CPs (averaged over $q < 0$ and $q > 0$), compared to the results of Eisenberger *et al.* [22] and to the results of QMC SJ ($\mathbf{q} \parallel [100]$) and LDA (orientational average). Inset: Zoom on the discontinuity (points) and the linear fits to the CP around p_F. Both runs give the same result within the error bars, the fits shown here are from run 2.

structure value in LDA, $|\tilde{\phi}^{\mathbf{G}=0}_{\nu=1,\mathbf{k}_F}|^2 = 0.98$, we deduce the experimental $Z_{k_F} = \zeta^{\mathrm{Na}}_{\mathrm{expt}}/|\tilde{\phi}^{\mathbf{G}=0}_{\nu=1,\mathbf{k}_F}|^2 = 0.58(7)$. We simulated the effect of the finite experimental q resolution by convoluting the QMC CP with the resolution function of run 2, and repeating the analysis described above. The result was an effective lowering of $\zeta^{\mathrm{Na}}_{\mathrm{QMC}}$ by 0.02, significantly smaller than our error bar of 0.07.

The $n(p)$ can be calculated from the experimental CP using Eq. (2) and is shown in Fig. 1. In the differentiation, the effect of statistical noise increases, and thus we only show the result after averaging the values of $p < 0$ and $p > 0$, as well as averaging adjacent measured points. Because of this, the quantitative determination of ζ is better done by directly analyzing the CP as described above. However, the trend of Table I is clearly seen also in Fig. 1, and the experimental $n(p)$ is consistent with the obtained $\zeta^{\mathrm{Na}}_{\mathrm{exp}}$.

We have also calculated the CP by QMC SJ for $\mathbf{q} \parallel [100]$ (Fig. 3); small differences with respect to the experiment remain. Further work is necessary to study if the inclusion of core electrons or phonon effects is necessary to reduce the residual discrepancy. In Fig. 1, we show the resulting direction-averaged $n(p)$. Finite-size corrections [21] are important to determine the structure around p_F, in particular, to obtain the jump at the FS, $\zeta^{\mathrm{Na}}_{\mathrm{QMC}} = 0.68(2)$. Within the QMC approach, we can determine bare band-structure effects by turning off the explicit electron-electron correlations in the underlying many-body wave function which yields a band-structure contribution $|\tilde{\phi}^{\mathbf{G}=0}_{\nu=1,\mathbf{k}_F}|^2 = 0.97(1)$ compatible with that of LDA. We therefore obtain $Z^{\mathrm{Na}}_{k_F} = 0.70(2)$, in agreement with QMC SJ calculations for HEG. More accurate QMC BF results on HEG indicate a slightly lower value, $Z^{\mathrm{HEG}}_{k_F} = 0.66(2)$.

From the G_0W_0 self-energy, we directly obtain $Z_{\mathbf{k}_F} = [1 - \partial\Sigma_{1,1}(\mathbf{k}_F, \omega)/\partial\omega|_{\omega=\epsilon_F}]^{-1} = 0.65(1)$. In order to determine the jump in $n(p)$, we further need the quasiparticle weight which, within G_0W_0, coincides with the Kohn-Sham orbital of the LDA calculation at the Fermi energy, and we get $\zeta^{\mathrm{Na}}_{G_0W_0} = 0.64(1)$. The $n(p)$ within G_0W_0 is very close to the QMC result.

The agreement between QMC BF and G_0W_0 results is remarkable. Furthermore, within both theories band-structure effects can be factorized from correlations within the accuracy of the calculation, which enables a direct comparison with HEG. In Table I, we summarize our experimental and theoretical results on $Z_{\mathbf{k}_F}$ and compare them to various theoretical results obtained for HEG. On theoretical grounds, QMC BF is considered to give the most precise result. Together with G_0W_0, it is in reasonable agreement with the experiment. Our experimental and theoretical values clearly exclude two different classes of approximation, and thus resolve a long-standing theoretical controversy. Whereas the so-called on-shell approximation of the RPA [4,5] leads to an underestimation of $Z_{\mathbf{k}_F}$, fully self-consistent GW calculations [6] overestimate its value. Interestingly, the use of the theoretically more appealing conserving approximation (GW) does not result in an improved description of spectral quantities compared to non-self-consistent (G_0W_0) treatments.

Conclusions.—We have determined the momentum distribution of Na valence electrons experimentally and theoretically. In particular, we have related the discontinuity at the Fermi level to the quasiparticle renormalization factor of HEG at $r_s = 3.99$, giving a long-sought reference value for this fundamental quantity.

Beam time was provided by the ESRF. The authors would like to thank Gy. Vankó, G. Monaco, R. Verbeni, H. Müller, and C. Henriquet (ESRF) for expert advice and assistance. J. A. S., T. P., and K. H. were supported by the Academy of Finland Contract No. 1127462. QMC work was supported by the U.S. DOE Grant No. DE-FG05-08OR2333, the INCITE program, and CNRS-IDRIS.

[1] P. Nozières, *Theory of Interacting Fermi Systems* (Benjamin, New York, 1964).
[2] L. Hedin, Phys. Rev. **139**, A796 (1965).
[3] T. M. Rice, Ann. Phys. (N.Y.) **31**, 100 (1965).
[4] E. Pajanne and J. Arponen, J. Phys. C **15**, 2683 (1982).
[5] J. Lam, Phys. Rev. B **3**, 3243 (1971).
[6] B. Holm and U. von Barth, Phys. Rev. B **57**, 2108 (1998).
[7] L. J. Lantto, Phys. Rev. B **22**, 1380 (1980).
[8] Y. Takada and H. Yasuhara, Phys. Rev. B **44**, 7879 (1991).
[9] W. M. C. Foulkes, L. Mitas, R. J. Needs, and G. Rajagopal, Rev. Mod. Phys. **73**, 33 (2001).
[10] C. Filippi and D. M. Ceperley, Phys. Rev. B **59**, 7907 (1999).
[11] *X-Ray Compton Scattering*, edited by M. J. Cooper *et al.* (Oxford University Press, Oxford, 2004).
[12] W. Schülke, G. Stutz, F. Wohlert, and A. Kaprolat, Phys. Rev. B **54**, 14 381 (1996).
[13] P. Suortti *et al.*, J. Phys. Chem. Solids **61**, 397 (2000).
[14] R. Verbeni *et al.*, J. Synchrotron Radiat. **16**, 469 (2009).
[15] A. Issolah, B. Lévy, A. Beswick, and G. Loupias, Phys. Rev. A **38**, 4509 (1988).
[16] J. J. Rehr and R. C. Albers, Rev. Mod. Phys. **72**, 621 (2000).
[17] J. A. Soininen, A. L. Ankudinov, and J. J. Rehr, Phys. Rev. B **72**, 045136 (2005).
[18] P. Holm, Phys. Rev. A **37**, 3706 (1988).
[19] J. A. Soininen, K. Hämäläinen, and S. Manninen, Phys. Rev. B **64**, 125116 (2001).
[20] C. Sternemann *et al.*, Phys. Rev. B **62**, R7687 (2000).
[21] M. Holzmann *et al.*, Phys. Rev. B **79**, 041308(R) (2009).
[22] P. Eisenberger, L. Lam, P. M. Platzman, and P. Schmidt, Phys. Rev. B **6**, 3671 (1972).